

Article

Carbon ($\delta^{13}\text{C}$) and Nitrogen ($\delta^{15}\text{N}$) Isotope Dynamics during Decomposition of Norway Spruce and Scots Pine Litter

Mukesh K. Gautam ^{1,2,*} , Björn Berg ³  and Kwang-Sik Lee ² 

¹ Biology Department, Medgar Evers College, City University of New York, New York, NY 11225, USA
² Research Center for Earth and Environmental Science, Korea Basic Science Institute, Cheongju-si 28119, Chungbuk, Republic of Korea; kslee@kbsi.re.kr
³ Department of Forest Sciences, University of Helsinki, 00014 Helsinki, Finland; bb0708212424@gmail.com
* Correspondence: mukeshcric@gmail.com

Abstract: We studied the dynamics of stable carbon ($\delta^{13}\text{C}$) and nitrogen ($\delta^{15}\text{N}$) isotopes in litter from Norway spruce (NSL) (*Picea abies*) and Scots pine (SPL) (*Pinus silvestris*) during in situ decomposition over a period of more than 4 years. Relative to initial values, $\delta^{13}\text{C}_{\text{NSL}}$ showed a weak enrichment (0.33‰), whereas $\delta^{13}\text{C}_{\text{SPL}}$ was depleted (−0.74‰) at the end of decomposition. Both litter types experienced a depletion in $\delta^{15}\text{N}$ during decomposition; $\delta^{15}\text{N}_{\text{NSL}}$ decreased by −1.74‰ and $\delta^{15}\text{N}_{\text{SPL}}$ decreased by −1.99‰. The effect of the selective preservation of acid-unhydrolyzable residue (AUR) in lowering $\delta^{13}\text{C}$ of the residual litter was evident only in SPL. In the NSL, only in the initial stage did C/N have a large effect on the $\delta^{13}\text{C}$ values. In the later stages, there was a non-linear decrease in $\delta^{13}\text{C}_{\text{NSL}}$ with a simultaneous increase in AUR concentrations, but the effect size was large, suggesting the role of lignin in driving $\delta^{13}\text{C}$ of residues in later stages. Depletion in $\delta^{15}\text{N}$ in the residual litters concomitant with the increase in N concentration suggests bacterial transformation of the litter over fungal components. A consistent decline in $\delta^{15}\text{N}$ values further implies that bacterial dominance prompted this by immobilizing nitrate depleted in $\delta^{15}\text{N}$ in the residual litter.

Keywords: litter decomposition; carbon isotope; nitrogen isotope; Scots pine; Norway spruce; boreal forests



Citation: Gautam, M.K.; Berg, B.; Lee, K.-S. Carbon ($\delta^{13}\text{C}$) and Nitrogen ($\delta^{15}\text{N}$) Isotope Dynamics during Decomposition of Norway Spruce and Scots Pine Litter. *Forests* **2024**, *15*, 1294. <https://doi.org/10.3390/f15081294>

Academic Editors: Zhenhong Hu, Chengjie Ren and Xingkai Xu

Received: 17 June 2024
Revised: 22 July 2024
Accepted: 22 July 2024
Published: 24 July 2024



Copyright: © 2024 by the authors. Licensee MDPI, Basel, Switzerland. This article is an open access article distributed under the terms and conditions of the Creative Commons Attribution (CC BY) license (<https://creativecommons.org/licenses/by/4.0/>).

1. Introduction

During the decomposition process, litter undergoes significant chemical transformations as it transitions from fresh litter to humus [1–6]. The stable isotope signatures of carbon ($\delta^{13}\text{C}$) and nitrogen ($\delta^{15}\text{N}$) and their discrimination during litter decomposition have helped provide insight into different aspects of chemical transformations, including carbon (C) and nitrogen (N) dynamics [7–12].

As decomposition proceeds and litter transitions through different phases involving two or three stages of chemical transformations, it becomes imprinted with characteristic isotopic ratios. These variations arise from a complex interplay of various factors [13–18]. Initially, litter decomposition is dominated by labile compounds over resilient ones [19]. As decomposition progresses and easily and moderately degradable compounds are broken down and leached out, the concentrations of recalcitrant organic matter—such as lignin or acid-unhydrolyzable residue (AUR)—and decay-resistant secondary compounds increase in the residual litter [4,8,19]. In the later stages, the ratio of the residual litter’s AUR, including its modified products, to the labile fraction is higher than in the initial stage. Incorporation of transformed carbon and nitrogen products of bacterial and fungal origin, or old stable C and N from underlying layers in the decomposing litter, alters the isotopic ratios of decomposing litter [20]. The nitrogen isotope ratio shows large changes due to various stages of nitrogen transformation, transfer, and assimilation linked to isotopic fractionation [21,22]. Loss of $\delta^{15}\text{N}$ -depleted labile N (through leaching, nitrification, and denitrification) and accumulation of $\delta^{15}\text{N}$ -enriched microbial biomass can increase the $\delta^{15}\text{N}$

of the litter [7,22–24]. However, bacterial dominance during decomposition can decrease ^{15}N signatures as bacteria have a greater potential for immobilizing nitrate depleted in ^{15}N in the residual litter [22,23,25,26]. In contrast, fungal dominance in decay processes can lead to an enrichment of ^{15}N in decomposing litter [27].

Subsequently, the isotopic signatures diverge from the initial litter due to constant transformation along with continuous accumulation or loss of transformed compounds. The most important factors influencing this process are AUR, the AUR/N ratio for $\delta^{13}\text{C}$, and organic-N fractionation for $\delta^{15}\text{N}$ during mineralization. AUR, being recalcitrant, is depleted in $\delta^{13}\text{C}$ by 2–6‰ compared to easily degradable ^{13}C -enriched compounds like sugars, starch, and cellulose [8,28,29]. Its selective preservation relative to easily degradable compounds in the decomposing litter, especially during the stable fraction stage (late stage), lowers the $\delta^{13}\text{C}$ values of residual litter [30–32]. Studies on $\delta^{13}\text{C}$ and $\delta^{15}\text{N}$ ratios during decomposition have shown diverse outcomes, such as enrichment [29,30], depletion [25,32,33], or negligible shifts in residual litter [9,33]. Some studies [7,8,11] have observed both depletion and enrichment in different litter species within the same region. The differences are likely related to the site conditions, which govern decomposition dynamics, species-specific characteristics, and the incubation time in the field. Various studies have provided important insight into the dynamics of carbon and nitrogen isotopes; still, only some isotopic changes are known. Also, these changes are limited to only a few litter types in certain ecosystems and generally on shorter timescales. Specific details of the chemical composition of litter, especially when the decomposition dynamics (accumulated mass loss) approach a limit value, or when concentrations of AUR or the AUR/N ratio change, have not been extensively studied [7,29]. For most foliar litter types and ecosystems, further investigations are needed, particularly on a long-term scale.

The primary objectives of this study were to elucidate (i) how $\delta^{13}\text{C}$ and $\delta^{15}\text{N}$ change during long-term (up to 60 months) decomposition of Norway spruce (*Picea abies*) and Scots pine (*Pinus silvestris*) litter and whether there is any litter-specific variability in dynamics between the two litter types; and (ii) how $\delta^{13}\text{C}$ and $\delta^{15}\text{N}$ dynamics are influenced by accumulated mass loss, AUR concentrations, and AUR/N ratios of the litter. The study, spanning up to 60 months, offers a comprehensive long-term analysis of stable isotopes during litter decomposition, exceeding the duration of several previous studies. By examining $\delta^{13}\text{C}$ and $\delta^{15}\text{N}$ stable isotopes, it provides detailed insight into the chemical transformations of Scots pine and Norway spruce litter during decomposition. The dual-isotope approach, their corresponding long-term isotopic changes, and the focus on AUR concentration and AUR/N ratio in the context of a hemiboreal forest provide a nuanced understanding of long-term litter decay dynamics unique to each species.

2. Materials and Methods

2.1. Study Site

The litter decomposition study was conducted in hemiboreal coniferous forest stands (site Grensholm) located in southeastern Sweden (58°33' N; 15°59' E, 58 m a.s.l.). The experimental site was dominated by paired monocultural stands of Norway spruce and Scots pine, aged 54 and 56, respectively. The boreal forest in Fennoscandia is dominated by two conifer species, Norway spruce (*Picea abies* L. Karst) and Scots pine (*Pinus sylvestris* L.), and both are of major importance for a wide range of forest ecosystem services, including litter decomposition. Norway spruce (50%) and Scots pine (30%) together account for 80% of forest biomass in Sweden. These two species are dominant in all the forests in Sweden. It is for this reason that we used these two species for this study. Both stands were growing on Eutric Cambisol, and the humus form was a mull. Further details about the site are given elsewhere [34,35].

2.2. Needle Litter Collection, Storage, and Mass-Loss Determination

For this study, we obtained litter samples of Scots pine (SPL) and Norway spruce (NSL) from the repositories developed by the late Dr. Maj-Britt Johansson along with

Dr. Björn Berg. Local needle litter was collected from both Norway spruce and Scots pine stands. Litter was collected in autumn of 1978 by gently shaking the branches of the trees and collecting the needles on spread-out tarpaulins. Green needles were removed by hand. Litter was air-dried and stored at room temperature. Before weighing, the needles were equilibrated to a constant moisture level ($5\%–8\% \pm 0.5\%$) by drying them at room temperature for about one month. The exact dry mass was determined by drying samples to a constant mass at $85\text{ }^{\circ}\text{C}$.

Litterbags, measuring $8 \times 8\text{ cm}$, excluding a 1 cm wide edge, were made of polyester net with a mesh size of about $1.0 \times 1.0\text{ mm}$ for pine needles and about $1.0 \times 0.5\text{ mm}$ for spruce needles. We placed 1.0 g (to 3 decimal places) of needle litter in each litterbag. The bags were deployed on the top of the litter (L) layer in 25 randomly located $1 \times 1\text{ m}$ spots within each plot in early May 1979. In each such spot, 10–14 bags were attached to the ground using pegs pushed through the edges of bags. Litterbags were incubated in situ for 5 and 4 years in the Norway spruce and Scots pine stands, respectively. Litterbags were retrieved from their respective sites after field incubation for 181, 369, 540, 736, 915, 1085, 1462, and 1833 days from the start of the experiment (June 1979 to May 1983). On each occasion, 25 litterbags per litter type were collected from each stand. The litterbags were gently brushed to remove new needles deposited on the bags and cleaned of residues such as through-growing plants like moss, grass, and plant roots. The bags were individually packed in brown-paper envelopes and transported to the laboratory. The bags were either stored at $-20\text{ }^{\circ}\text{C}$ (if storage was needed) or cut open immediately to air-dry the litter sample and clean the litter of any ingrown foreign material (moss, grass, and plant roots). Litter samples were then dried at $85\text{ }^{\circ}\text{C}$ until they achieved constant weight (about 2 days). The dried samples were allowed to cool in a desiccator before weighing and the exact litter weight of each bag was recorded with an accuracy of two decimal places. Mean values of mass loss were calculated for each sample set of 25 bags, and details are given in Berg et al. [36]. Following air-drying to an even moisture level, samples were thoroughly dried ($85\text{ }^{\circ}\text{C}$). They were then ground into fine powder, sealed, and stored in air-tight containers at room temperature. Ground samples stored in a dark and dry environment have indefinite storage life and samples can be left for any length of time in clean air-tight conditions Jones et al. [37] and Kalra et al. [38]. This way, samples' integrity is maintained for follow-up analytical work [39]. The biplot of old and new nitrogen analysis shows high correlation ($r = 0.97$), and a standardized U value of zero means that there is no statistically significant difference between the two samples according to the Mann–Whitney U test ($U_{\text{standardized}} = 0.0$; $p = 0.95–0.32$) (Supplementary Figure S1). Thoroughly dried, ground litter samples were sealed and stored dry at room temperature until retrieved from storage in April 2021. Litterbag data (data on accumulated mass loss) and AUR (gravimetric lignin) were taken from Berg et al. [40].

2.3. Sample Preparation and Chemical Analyses

To prepare homogenized samples for determining the concentrations of carbon and nitrogen and their isotope values, the ground litter samples were first freeze-dried at $-80\text{ }^{\circ}\text{C}$ for 96 h and then ground again into a fine powder using an agate ball mill (MM400; Retsch, Haan, Germany) at Korea Basic Science Institute (KBSI), Korea, and stored in glass vials. Litter C and N concentrations were determined by combusting samples at $1100\text{ }^{\circ}\text{C}$ in a Flash EA Elemental Analyzer (1112 Series, Thermo Electron S.p.A., Rodano, Italy) at the Korea Basic Science Institute, Korea.

To determine the C and N isotope ratios, about 0.1 mg and 8 mg of the samples, respectively, were enclosed in different tin containers ($3.5 \times 1.5\text{ mm}$; Elemental Microanalysis, Okehampton, UK). Until further analysis, the samples enclosed in tin containers were stored in a desiccator to prevent vapor absorption. C and N isotope ratios were determined using an isotope ratio mass spectrometer (IRMS; VisION, Isoprime Ltd., Manchester, UK) equipped with a vario PyroCube elemental analyzer (Elementar, Hesse, Germany). The elemental analyzer included a combustion tube maintained at $1150\text{ }^{\circ}\text{C}$, which was oper-

ated in continuous flow mode. The encapsulated sample was combusted at 1150 °C in a combustion reactor, and any excess oxides were subsequently removed in a reduction reactor maintained at 850 °C. Afterwards, the N₂ and CO₂ gases generated were separated through chromatography, and the isotope ratios were measured using the IRMS (VisION, Isoprime Ltd., Manchester, UK). Because of varying content of C and N in samples, C and N isotopes were analyzed separately. Stable isotope ratios were reported using the standard delta notation (δ) relative to an international standard unit per mil (‰) as follows: δ (‰) = $(R_{\text{sample}}/R_{\text{reference}} - 1) \times 1000$, where R_{sample} and $R_{\text{reference}}$ are the molar ratios of the heavy to light isotopes of the sample and standard, respectively, representing $^{13}\text{C}/^{12}\text{C}$ or $^{15}\text{N}/^{14}\text{N}$. The resulting $\delta^{13}\text{C}$ and $\delta^{15}\text{N}$ values were reported against Vienna Pee Dee Belemnite (VPDB) and atmospheric nitrogen (air), respectively. The analytical precision was within $\pm 0.1\text{‰}$ for C and N isotopes. The following standard reference materials were used for the calibration of C and N isotope ratios: NBS-22 (oil, $\delta^{13}\text{C}_{\text{VPDB}} = -29.8\text{‰}$), IAEA-CH-3 (cellulose, $\delta^{13}\text{C}_{\text{VPDB}} = -24.73\text{‰}$), IAEA-CH-6 (sucrose, $\delta^{13}\text{C}_{\text{VPDB}} = -10.45\text{‰}$), IAEA-600 (caffeine, $\delta^{13}\text{C}_{\text{VPDB}} = -27.77\text{‰}$, $\delta^{15}\text{N}_{\text{Air}} = +1.0\text{‰}$), USGS-40 (l-glutamic acid, $\delta^{13}\text{C}_{\text{VPDB}} = -26.39\text{‰}$, $\delta^{15}\text{N}_{\text{Air}} = -4.52\text{‰}$), and IAEA-NO₃ (potassium nitrate, $\delta^{15}\text{N}_{\text{Air}} = +4.7\text{‰}$).

2.4. Data Analyses

The decomposition patterns and rates were estimated using the accumulated mass loss (AML) or remaining amount (or concentrations for elements) of litter using the single exponential model: $\ln(M_t/M_0) = -k_t$, where M_0 is the initial mass at time t_0 , M_t is the mass at a certain time in the decomposition period, t (year), and k is the decay rate constant (yr^{-1}) [5,41]. We calculated the asymptotic limit values for decomposition and the decomposition rate (k_A) according to Wieder and Lang [42] and Berg and Ekbohm [43]:

$$L_t = m (1 - e^{-k_A t/m})$$

where L_t is the accumulated mass loss (in percent), t is time in days, k_A is the decomposition rate at the beginning of the decay, and m represents the asymptotic level that the accumulated mass loss will ultimately reach.

The per mil (‰) fractionation factor (Δ) was calculated to estimate the difference in C and N isotopic compositions between the residues at the start (t_0 initial) and the end (t_f final) of decomposition [44].

To compare the dynamics in the litter types and emphasize temporal differences in concentration and amount against time and AML, line plots were used. The trends generated in the plots allowed us to perceive the distinctive pattern of change. We used polynomial regression (linear and quadratic models) to test the relationships between element dynamics and AML. Two separate regression analyses were run, one with the change in element concentration vs. time and another with percent AML of the decomposing litter to determine the underlying relationship. If a linear relationship was not fitting the data and unable to capture the patterns, a polynomial quadratic regression was used to model the relationship between variables to match the pattern of the data, $Y = \text{Pr}_1 + \text{Pr}_2 X + \text{Pr}_3 X^2$, where Y represents the element concentrations, Pr_1 is the intercept, and Pr_2 and Pr_3 are estimates of parameters of quadratic regression for AML. To quantify the strength of the effect that these predictors have on the isotopic composition, Cohen's f^2 statistic was used: $f^2 = R^2 / (1 - R^2)$, where R^2 represents the coefficient of determination. Generally, a larger f^2 value (>0.35) indicates a large effect size and hence a stronger relationship between the variables. Effect sizes are medium and small when f^2 falls between 0.15 and 0.34 and below 0.02, respectively. Pearson correlation was used to study relationships among various variables recorded during the decomposition. XLSTATpro (v 13.2.1.0) was used for the statistical analyses and graphical visualizations (Addinsoft, New York, NY, USA). Equality of slopes of regression was estimated using LINEST and slope test syntax in MS Excel.

3. Results

3.1. Initial Litter at Time t_0

Scots pine needles (SPL) had low concentrations of carbon and AUR compared to Norway spruce needles (NSL). In contrast, nitrogen concentration was slightly higher in the SPL relative to NSL (Figure 1). The C/N and AUR/N ratios of NSL were higher in comparison to those of SPL. Relative differences, however, between the two litter types were small. In terms of stable isotope ratios, NSL was depleted in ^{13}C compared to SPL by 0.09‰, whereas NSL was enriched in ^{15}N relative to SPL by 0.27‰ (Figure 1).

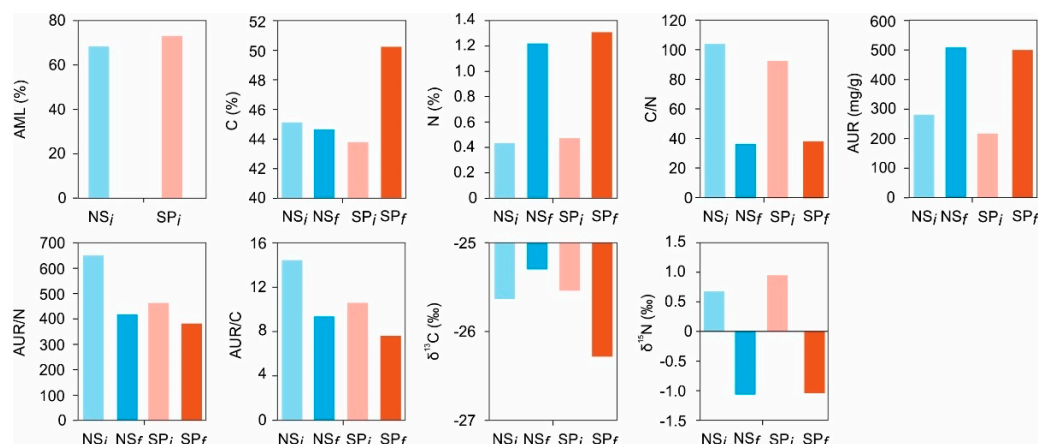


Figure 1. Initial and final concentrations of C, N, and AUR as well as the ratios for C/N and AUR/N. Their C ($\delta^{13}\text{C}$) and N ($\delta^{15}\text{N}$) isotopic compositions are given. NSL and SPL are Norway spruce and Scots pine litter types, respectively. The subscripts i and f denote initial and final litters. AML is accumulated mass loss, and AUR is acid-unhydrolyzable residue.

3.2. Litter Mass Loss and Decomposition Dynamics

During decomposition, litter undergoes significant chemical transformations from fresh litter to humus, influenced by various factors including the balance of labile and recalcitrant compounds and microbial activity [1,17,19,32]. As decomposition progresses, labile compounds break down first, leaving behind more recalcitrant compounds such as lignin, which impacts the chemical and isotopic composition of the remaining litter. These changes are reflected in the residual litter, which provides insights into the underlying biochemical processes [3,4,11,19].

The relationships between percentage AML and time resulted in a good fit ($R^2 \geq 0.95$) (Figure 2a). AML was higher for SPL (42%) than for NSL (19%) in the first year. NSL took more than twice the time compared to SPL to achieve an equivalent AML. After one year, the AML rate declined, with SPL decreasing faster than NSL (Figure 2b). SPL consistently had higher AML than NSL (Figure 2b). After about four years of in situ decomposition, SPL began to plateau, asymptotically approaching a limit value of 74.4% AML. Conversely, after 5 years and 68% mass loss, NSL's AML still decreased, suggesting that a longer incubation would be needed for NSL to reach the limit value of 92.2% AML.

Decay rates differed between the two species. The annual k decay constant suggested higher decomposition rates for SPL in terms of C and AUR as well as a higher N loss rate compared to NSL (Table 1). The equality of slopes test ($p < 0.05$) showed significant differences in the decay rates (heterogeneity in slope), with steeper slopes for SPL up to about 75% AML. SPL's decay rate decreased less rapidly near the limit value, whereas NSL maintained a relatively steady decay rate (approaching an asymptote) throughout the observation period. Loss rates of C, N, and AUR also differed between the two litter types (Figure 2).

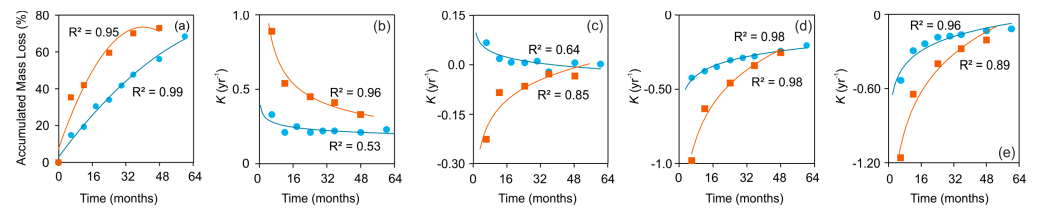


Figure 2. Accumulated mass loss (%) plotted against time (months) in biplot (a), and decomposition rate constant (k_s) vs. time in biplot (b). Decomposition rate constants (k_s) for carbon vs. time (c). Rate constants (k_s) for loss of N (d) and rate constants (k_s) for loss of AUR (e). Litter are needle litter of Norway spruce (blue circle) and Scots pine (red square), respectively.

Table 1. Overall annual decay rate constant ($k_s \text{ yr}^{-1}$) for needle litters of Norway spruce (NSL) and Scots pine (SPL). The k_s was calculated for the whole in situ decomposition period. The Δ is the difference between initial and final litter isotopic ratios (in per mil ‰).

	NSL		SPL
		$k_s \text{ yr}^{-1}$	
AML	0.22		0.32
C	0.002		−0.031
N	−0.21		−0.25
AUR	−0.12		−0.21
$\delta^{13}\text{C}$	0.003		−0.007
$\delta^{15}\text{N}$	0.09		0.02
		Δ (‰)	
$\Delta^{13}\text{C}$ (‰)	0.33		−0.74
$\Delta^{15}\text{N}$ (‰)	−1.74		−1.99

3.3. $\delta^{13}\text{C}$ Dynamics during Decomposition

The $\delta^{13}\text{C}_{\text{NSL}}$ values fluctuated narrowly, ranging from -25.63‰ to -25.30‰ (Figure 3). After a decline between 12 and 24 months (from -25.06‰ to -25.78‰), NSL's $\delta^{13}\text{C}$ values remained relatively stable, ending at -25.30‰ after 5 years, showing slight enrichment (Figure 3a). SPL's $\delta^{13}\text{C}$ values ranged from -25.65‰ to -26.28‰ . The $\delta^{13}\text{C}$ values for SPL showed a declining trend overall, suggesting a shift towards depletion during the decomposition. After 48 months, SPL's lowest value was -26.28‰ , indicating significant depletion. Comparing $\delta^{13}\text{C}_{\text{NSL}}$ and $\delta^{13}\text{C}_{\text{SPL}}$, NSL showed more fluctuations, reflecting dynamic enrichment and depletion, whereas SPL exhibited relatively stable $\delta^{13}\text{C}$ values, indicating minimal fluctuations.

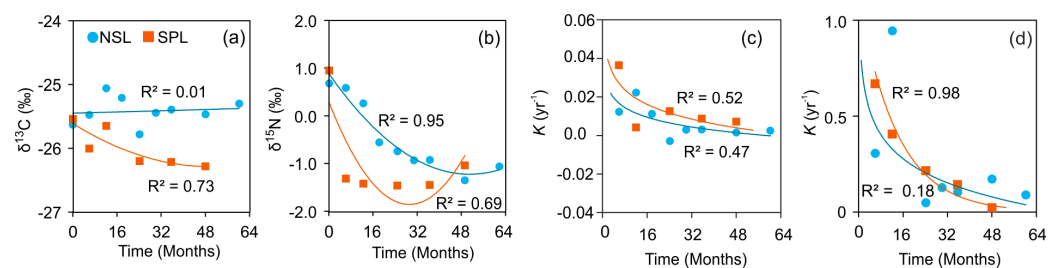


Figure 3. Carbon ($\delta^{13}\text{C}$) (a) and nitrogen $\delta^{15}\text{N}$ (b) over time and their decay rates ($k \text{ yr}^{-1}$) dynamics through time (c,d), respectively, during in situ decomposition of local needle litters of Norway spruce (blue circle) and Scots pine (red square).

The regression fit parameter of $\delta^{13}\text{C}$ against AML showed a significant relationship only for the SPL ($R^2 = 0.80$; $p < 0.05$) and not for that of NSL ($R^2 = 0.03$; $p = \text{ns}$) (Figure 4a). The same trend was seen for the change in carbon concentration (Figure 4b). For NSL, linear or quadratic terms for other variables (C, N, C/N, AUR, AUR/C, and AUR/N) were

not statistically significant predictors of $\delta^{13}\text{C}$ dynamics ($R^2 = 0.01\text{--}0.13$, p -values > 0.05). However, the polynomial quadratic regressions showed moderate to high explanatory power ($R^2 = 0.67\text{--}0.79$) for $\delta^{13}\text{C}_{\text{SPL}}$, indicating these variables' role in carbon isotopic variability. SPL peaks at approx. 60% AML, shifting from an increase to a decrease (Figure 4g). The model fitted the data reasonably well, and N, C/N, and AUR are the individual predictors which significantly explain variation in $\delta^{13}\text{C}_{\text{SPL}}$.

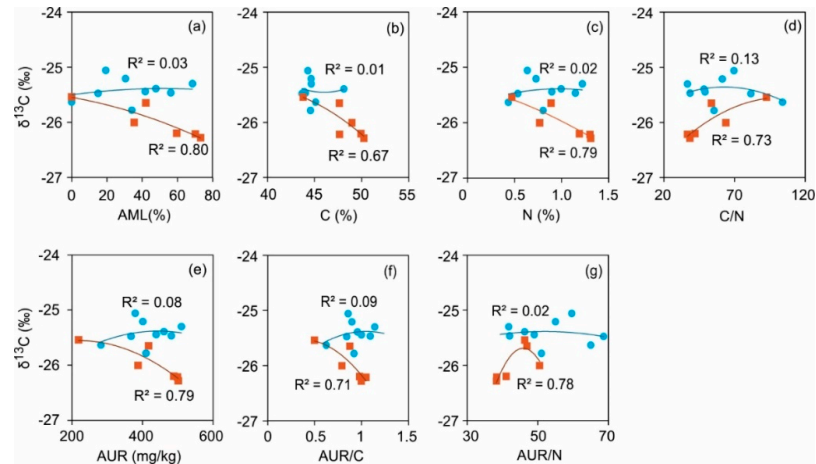


Figure 4. Fitted regression plots between change in $\delta^{13}\text{C}$ (‰) with accumulated mass loss (%) and changes in C, N, and AUR concentrations as well as the ratios C/N, AUR/C, and AUR/N as predictor variables for decomposing litter of local Norway spruce (NSL) and Scots pine (SPL) in hemiboreal forest stands, site Grensholm Castle, Southern Sweden. Circle (blue) and Square (red) represent Norway spruce and Scots pine litter, respectively.

3.4. $\delta^{15}\text{N}$ Dynamics during Decomposition

Initially, NSL exhibited a $\delta^{15}\text{N}$ value of 0.68‰, indicating slight enrichment. Over time, $\delta^{15}\text{N}$ values decreased to -1.35 ‰ at the 4-year mark and slightly increased to -1.07 ‰ after 5 years, suggesting $\delta^{15}\text{N}_{\text{NSL}}$ depletion (Figure 5b). In contrast, $\delta^{15}\text{N}_{\text{SPL}}$ fluctuated, starting at 0.95‰, decreasing to -1.45 ‰ at the 24.1-month mark, and recovering to -1.04 ‰ after 4 years. Both litter types experienced $\delta^{15}\text{N}$ depletion, but NSL exhibited a more consistent and pronounced depletion trend compared to SPL's variability.

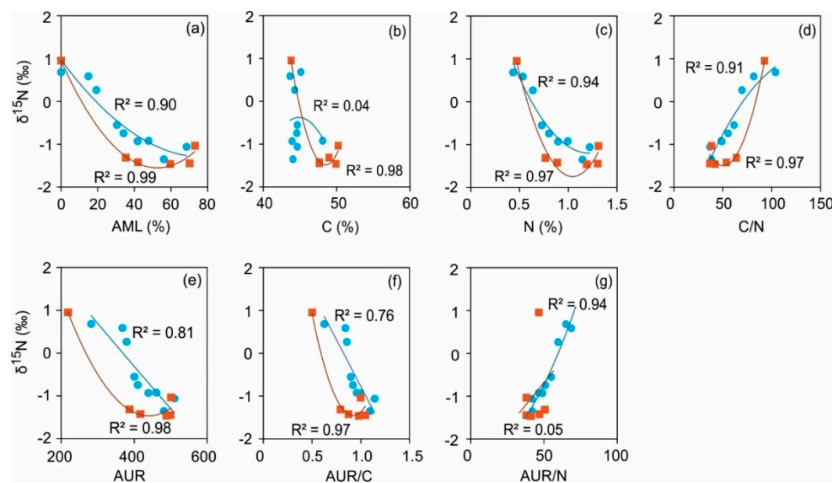


Figure 5. Fitted plots of regressions between $\delta^{15}\text{N}$ (‰) change and accumulated mass loss (%) and other predictor variables for decomposing litter of local Norway spruce (NSL) and Scots pine (SPL) in hemiboreal forest stands, site Grensholm Castle, Southern Sweden. Circle (blue) and Square (red) represent Norway spruce and Scots pine litter, respectively.

The AML is a significant predictor of $\delta^{15}\text{N}$ for both NSL and SPL, indicated by high R^2 (0.90–0.99) and low p -values (<0.05) (Figure 5a). Polynomial regressions suggest a non-linear relationship where $\delta^{15}\text{N}$ decreases as AML increases (Figure 5a). C, N, C/N, AUR, AUR/C, and AUR/N also showed strong fits ($R^2 = 0.76$ – 0.99 ; $p < 0.05$), suggesting their effects on $\delta^{15}\text{N}$ dynamics of both litter types (Figure 5b–g).

4. Discussion

4.1. Comparison of Change in $\delta^{13}\text{C}$ with Previous Studies

The divergence in $\delta^{13}\text{C}$ dynamics between the two litter types is noticeable. Similar to Connin et al. [7], we noticed both enrichment and depletion in our litter types. NSL experienced enrichment, similar to previous studies [29,30]. Its $\delta^{13}\text{C}$ dynamics was two-phased, initially showing enrichment in the first few months before undergoing depletion, reaching an asymptote after the 16th month. Conversely, SPL showed a single-phase decline in $\delta^{13}\text{C}$, with faster depletion in the early stage, reconciling with previous studies [7,8,33]. Contrary to our observation, other researchers [9,34] have reported negligible shifts in the $\delta^{13}\text{C}$ values of the residual litter. This is likely due to the shorter incubation period employed in these studies. The later phases of both litter types exhibited more stable isotopic shifts, suggesting that isotopic discrimination is primarily determined during the initial decay phases [7]. The overall dynamics and asymptote align with $\delta^{13}\text{C}$ changes against AML and decay rate over time, particularly in later stages. The relationship, however, was significant only in SPL, especially against AML.

4.2. Factors Influencing $\delta^{13}\text{C}$ Signatures of Decomposing Litter

The different isotopic shifts for the two litters suggest that different processes are involved in the shift in $\delta^{13}\text{C}$ values of the residual litter. To determine if changes in carbon concentrations are related to an increase in $\delta^{13}\text{C}$, we regressed both of them. For NSL, no significant relationship was found, with very low Cohen's f^2 effect sizes (0.01–0.15). At 68.5% AML, the change in carbon concentration of NSL was negligible, showing a 0.01-fold decrease from the initial value, which occurred only in the initial month. This infinitesimal change in carbon concentration over 5 years cannot account for the observed increase in $\delta^{13}\text{C}$ during decomposition. A shift in $\delta^{13}\text{C}$ towards a less negative value over time is generally tied to fungal- or bacteria-mediated transfer of ^{13}C -enriched fractions from the decaying environment to residual litter, or the incorporation of microbial biomass into the decaying litter [29,45,46]. It was also suggested that this increase may be related to the preferential utilization by microbes and subsequent loss of ^{12}C -enriched soluble fractions from the decomposing litter during transformation [7]. Fungal biomass is known to be enriched in ^{13}C compared to intact foliar components [46,47]. The loss of ^{13}C -depleted lignin or lignin-like compounds can increase the isotope signatures of residual litter [8]. In our study, we found an insignificant relationship between $\delta^{13}\text{C}$ and AUR. The AUR in NSL showed a 1.81-fold increase compared to the initial value, suggesting the preservation of lignin or lignin-like compounds. No significant relationships were found between $\delta^{13}\text{C}_{\text{NSL}}$ and other parameters (N, C/N, AUR/N), with very low Cohen's f^2 , demonstrating a miniscule to non-existent effect of these parameters on $\delta^{13}\text{C}$ values. The fractionation from substrate breakdown and CO_2 release during microbial respiration can also affect the isotopic composition of residual litter [48,49]. As CO_2 , depleted in ^{13}C , is respired during microbial respiration, the subsequent isotopic fractionation alters the initial litters' isotopic values [50,51]. Preferential utilization and loss of ^{12}C during microbial respiration can result in the enrichment of residual matter in ^{13}C [52].

The depletion observed in SPL can primarily be attributed to site-specific spatial heterogeneity between NSL and SPL stands. Variations in microbial biomass, their succession during decomposition, and differences in litter fraction utilization and transformation rates contribute to the $\delta^{13}\text{C}$ disparities [11,53]. The decrease in $\delta^{13}\text{C}$ values is associated with the selective preservation and accumulation of lignin or similar organic molecules in the residual litter [32,54,55]. Lignin, which is depleted by -4% to -7% in ^{13}C relative to easily

degradable labile carbon pools, plays a significant role in this process [55]. The $\delta^{13}\text{C}_{\text{SPL}}$ decrease is correlated with an increase in AUR concentration, underscoring lignin's role in decreasing $\delta^{13}\text{C}$ values of litter, especially in the advanced stages of litter decomposition. Similarly, NSL experienced increased AUR concentration, although the $\delta^{13}\text{C}$ –AUR relationship is not significant. If AUR overwhelmingly defines the $\delta^{13}\text{C}$ of litters during advanced decomposition, both litters would exhibit depleted isotopic values, but that was not observed. These results suggest that the role of lignin in $\delta^{13}\text{C}$ values is co-dependent on other factors.

Both AUR concentration and its decay rate (k_s) increased continuously until a mass loss of approx. 60% was reached, followed by limited change (Figure 2e). In the early stages, SPL exhibited faster and higher AML and decay rate (k_s) relative to NSL. The heterogeneity of slopes resulted in significant differences between AML and decay rate dynamics of both litter types. This implies that SPL had a higher degradation rate of polysaccharides early on. Furthermore, AUR either became stabilized, or its decomposition was lagging or limited [56]. The increase in AUR concentration is associated with an increase in carbon concentration, suggesting co-preservation in SPL ($R = 0.86$; $p < 0.05$) (Supplementary Figure S2). This is probably the carbon that was tightly bound to highly recalcitrant AUR or lignin–carbohydrate complexes or other organic molecules, which are ^{13}C -depleted [8,19]. Berg and Staaf [57] reported a decrease in cellulose and hemicellulose while lignin and nitrogen increased. The selective consumption by microbes and subsequent loss of polysaccharides (cellulose and hemicellulose), especially during the initial stages, presumably shifted the C isotope composition of the residual litter to being more negative.

The enrichment of nitrogen leads to an increase in AUR concentration within decomposing residues [19,58,59]. This happens through the effect of N in suppressing or decreasing the formation of fungal lignolytic enzymes, which are responsible for mediating lignin breakdown [56,60,61]. Also, a direct incorporation of N compounds in lignin may take place as discussed by Berg and McClaugherty [19]. We observed significant negative correlations of nitrogen and lignin concentration with the decrease in the decay rate (k_s) of SPL ($r = -0.90$) (Table 2). Additionally, a direct relationship was observed between increases in the concentrations of nitrogen and lignin ($R^2 \geq 0.98$) (Figure S3). This relationship was significant in both litter types. However, only in the SPL, both nitrogen and lignin (AUR) showed significant relationships with $\delta^{13}\text{C}$. Probably, in SPL, this is a nonlabile form of nitrogen that is bound to lignin which is retained during litter decomposition [62].

Table 2. Correlation matrix showing Pearson's correlation coefficients (R) of decay rate (k_s) with other variables for decomposing litter of local Norway spruce (NSL) and Scots pine (SPL) in hemiboreal forest stands, site Grensholm Castle, Southern Sweden. Superscript asterisk (*) next to correlation coefficient shows significant correlation at p -value ≤ 0.05 . AML, C, N, and AUR are accumulated mass loss, carbon, nitrogen, and acid-unhydrolyzable residue.

	AML	C	N	AUR	C/N	AUR/N
$k_{s\text{NSL}}$	−0.49	−0.27	−0.54	−0.48	0.67 *	0.72 *
$k_{s\text{SPL}}$	−0.89 *	−0.18	−0.90 *	−0.91 *	0.94 *	0.92 *

4.3. Comparison of Change in $\delta^{15}\text{N}$ with Previous Studies

According to ANOVA, both NSL and SPL experienced significant $\delta^{15}\text{N}$ depletion relative to initial isotopic values during decomposition. NSL exhibited a more consistent depletion compared to SPL, which showed slight enrichment towards the study's end. The $\delta^{15}\text{N}$ depletion observed in our study aligns with previous studies [6,25]. Bragazza et al. [26] found both depletion and enrichment among various litter species collected from a 2 ha Marcesina bog. Other studies have reported $\delta^{15}\text{N}$ enrichment during decomposition [7,10,21]. The differences likely stemmed from variations in litter species and site-specific factors. Overall, both litter types experienced single-phase depletion with

AML. $\delta^{15}\text{N}$ decline was more rapid in SPL than in NSL. In the initial years, SPL showed a greater magnitude of decrease compared to NSL, with SPL decreasing ~250% and NSL ~62% in the first year. At the same time, SPL's AML was twice that of NSL. NSL took an additional 1.5 years of incubation to match SPL's magnitude of the initial percent decrease.

4.4. Factors Influencing $\delta^{15}\text{N}$ Signatures of Decomposing Litter

The negative coefficients of regression for nitrogen concentration indicate an inverse relationship with $\delta^{15}\text{N}$, suggesting that higher nitrogen concentration leads to lower nitrogen isotopic ratios. The regression showed high explanatory power ($R^2 > 0.93$). The robust $\delta^{15}\text{N}$ -to-N concentration relationship across litter types suggests nitrogen's crucial role in determining $\delta^{15}\text{N}$ in litter. Possible explanations for the observed depletion include interactions between nitrogen availability, microbial processing, and isotopic fractionation within the litter decomposition continuum [7,20,22,26,63]. Nitrogen concentrations differed significantly between initial and final values, increasing by more than 175% for both litter types, suggesting immobilization and enrichment of residual litter with nitrogen. Melillo et al. [25] noted a correlation between $\delta^{15}\text{N}$ decrease and nitrogen immobilization. Similar to our study, they too recorded a depletion in $\delta^{15}\text{N}$ values by 2–3‰ during the immobilization phase.

There was a significant relationship between $\delta^{15}\text{N}$ values and AML ($R^2 > 0.90$). The depletion of $\delta^{15}\text{N}$ probably resulted from microbial activity [21,26,64]. Various studies suggest that changes in bacteria-to-fungi ratios in the decaying environment can either increase or decrease the $\delta^{15}\text{N}$ values [22,23,25–27]. Decomposition driven primarily by bacteria can decrease $\delta^{15}\text{N}$ signatures due to discrimination and biological fractionation during nitrogen transformations [23,25]. Bacteria have a greater potential for immobilizing nitrate depleted in ^{15}N in the residual litter [22,23,26]. Nitrification of ammonium can lead to a decrease in the $\delta^{15}\text{N}$ due to discrimination against the heavier nitrogen isotope (^{15}N) by both ammonia-oxidizing bacteria and nitrite-oxidizing bacteria [22]. The $\delta^{15}\text{N}$ values are particularly sensitive to the fractionation effects during nitrification, which tends to decrease their values [22,23]. In contrast, dominance of fungi can lead to an enrichment of ^{15}N in decomposing litter [27]. Although we did not investigate bacterial and fungal biomass in our study, the decrease in $\delta^{15}\text{N}$ of NSL and SPL during decomposition may be largely mediated by bacterial biomass. A study by Bragazza et al. [26] reported a similar observation in sedge and grass litter.

We recorded a significant relationship between $\delta^{15}\text{N}$ and C:N ratios ($R^2 > 0.90$) (Figure 5d) and between C:N ratios and AML ($R^2 > 0.92$). As AML increased, nitrogen concentration increased relative to carbon, depleting residual litter in ^{15}N . The decrease in the C:N ratio is primarily due to increased nitrogen, with a limited increase in carbon. Low C:N ratios lead to intense bacterial activity and their increased biomass. The decrease in C:N ratios in the residual litter indicates conditions conducive to bacterial dominance over fungal colonization [26,64]. Bacteria preferentially assimilate $\delta^{15}\text{N}$ -depleted nitrogen, possibly decreasing $\delta^{15}\text{N}$ values in remaining litter. Indirectly, the dominant bacterial role is suggested by the increased AUR concentration with AML in the residual litter. Nitrogen availability influences the composition and activity of microbial communities. High nitrogen levels can increase AUR concentration by suppressing the population and activity of lignin-degrading fungi and inhibiting lignolytic enzymes' production (i.e., peroxidases and laccases) by fungi [36,60,61]. The observed decrease or lack of change in $\delta^{13}\text{C}$ values supports that $\delta^{15}\text{N}$ values are modulated by bacteria rather than fungi in both NSL and SPL. We also noticed a significant relationship between $\delta^{15}\text{N}$ and AUR, with a high Cohen's f^2 effect (>3.17). Overall, the decrease in $\delta^{15}\text{N}$ with increasing AUR and nitrogen concentration suggests a complex interplay between nitrogen availability, microbial community dynamics, and isotopic fractionation processes during decomposition.

5. Conclusions

The dynamics of $\delta^{13}\text{C}$ and $\delta^{15}\text{N}$ isotopes during litter decomposition in hemiboreal forest stands reveal complex interactions influenced by litter type and environmental factors. The $\delta^{13}\text{C}$ values of NSL and SPL litter exhibited distinct patterns, with NSL experiencing overall enrichment and SPL showing depletion, reflecting the interplay of microbial processes and litter composition. Regression analyses indicated that AML significantly predicted $\delta^{13}\text{C}$ and $\delta^{15}\text{N}$ dynamics, highlighting the importance of bacterial activity and litter transformation rates in isotopic fractionation. This effect was modulated by AUR and nitrogen concentrations. Similarly, the $\delta^{15}\text{N}$ values showed depletion over time. The relationship between $\delta^{15}\text{N}$ and nitrogen concentration, C:N ratio, and AML underscored the influence of microbial community dynamics and nitrogen availability on isotopic fractionation processes during decomposition. Notably, the decrease or lack of change in $\delta^{13}\text{C}$ and consistent depletion of $\delta^{15}\text{N}$ during litter decomposition, along with increased AUR and nitrogen concentrations, support that the decomposition rate decreases and its effects on isotopic values are modulated by bacteria rather than fungi in both NSL and SPL litter. Overall, these findings contribute to better understanding of litter decomposition processes and the underlying mechanisms driving isotopic dynamics in forest ecosystems.

Supplementary Materials: The following supporting information can be downloaded at <https://www.mdpi.com/article/10.3390/f15081294/s1>: Figure S1. Biplots showing the high correlation between N (%) from old analysis (N_{old}) and N (%) from this study (N_{new}) in decomposing litter of local Norway spruce (NSL) (a) and Scots pine (SPL) (b) in hemi-boreal forest stands, site Grensholm Castle, Southern Sweden. Figure S2. Pearson correlation matrix showing relationships among accumulated mass loss (AML) (%), carbon (%), nitrogen (%), AUR (mg/g), C/N, AUR/N and AUR/C for decomposing litter of local Norway spruce (NSL) (green lower panel) and Scots pine (SPL) (upper red panel) in hemi-boreal forest stands, site Grensholm Castle, Southern Sweden. R is correlation coefficient and P is significance value at ≤ 0.05 . Figure S3. Biplot showing the significant relationship between N and AUR concentrations in decomposing litter of local Norway spruce (NSL) and Scots pine (SPL) in hemi-boreal forest stands, site Grensholm Castle, Southern Sweden.

Author Contributions: B.B. collected the data from field explorations. M.K.G. and K.-S.L. analyzed the samples. M.K.G., B.B. and K.-S.L. processed and analyzed the data. M.K.G., B.B. and K.-S.L. wrote the paper. K.-S.L. provided analytical and other logistic support for the study. K.-S.L. provided the funding for the study. All the authors contributed to the article and approved the submitted version. All authors have read and agreed to the published version of the manuscript.

Funding: This study was supported by the Korea Basic Science Institute (KBSI) grant (A425100).

Data Availability Statement: The data can be made available on request to Björn Berg and Mukesh K. Gautam.

Acknowledgments: The authors are thankful to the Late Maj-Britt Johansson who designed the experiment and executed the main part of the experiments. Furthermore, she provided litter samples from her repository for this study.

Conflicts of Interest: The authors declare that this research was conducted in the absence of any commercial or financial relationships that could be construed as potential conflicts of interest.

References

1. Berg, B.; Laskowski, R. *Litter Decomposition, a Guide to Carbon and Nutrient Turnover*; Elsevier: New York, NY, USA, 2005.
2. Balesdent, J.; Girardin, C.; Mariotti, A. Site-related $\delta^{13}\text{C}$ of tree leaves and soil organic matter in a temperate forest. *Ecology* **1993**, *74*, 1713–1721. [[CrossRef](#)]
3. Kelleway, J.J.; Trevathan-Tackett, S.M.; Baldock, J.; Critchley, L.P. Plant litter composition and stable isotope signatures vary during decomposition in blue carbon ecosystems. *Biogeochemistry* **2022**, *158*, 147–165. [[CrossRef](#)]
4. Rubino, M.; Lubritto, C.; D'Onofrio, A.; Terrasi, F.; Gleixner, G.; Cotrufo, M.F. An isotopic method for testing the influence of leaf litter quality on carbon fluxes during decomposition. *Oecologia* **2007**, *154*, 155–166. [[CrossRef](#)] [[PubMed](#)]
5. Ding, Y.; Wang, D.; Zhao, G.; Chen, S.; Sun, T.; Sun, H.; Wu, C.; Li, Y.; Yu, Z.; Li, Y.; et al. The contribution of wetland plant litter to soil carbon pool: Decomposition rates and priming effects. *Environ. Res.* **2023**, *224*, 115575. [[CrossRef](#)]

6. Gautam, M.K.; Berg, B.; Lee, K.S.; Nilsson, T.; Shin, H.S. Dynamics of trace and rare earth elements during long-term (over 4 years) decomposition in Scots pine and Norway spruce forest stands, Southern Sweden. *Front. Env. Sci.* **2023**, *11*, 1190370. [[CrossRef](#)]
7. Connin, S.L.; Feng, X.; Virginia, R.A. Isotopic discrimination during long-term decomposition in an arid land ecosystem. *Soil Biol. Biochem.* **2001**, *33*, 41–51. [[CrossRef](#)]
8. Osono, T.; Takeda, H.; Azuma, J.I. Carbon isotope dynamics during leaf litter decomposition with reference to lignin fractions. *Ecol. Res.* **2008**, *23*, 51–55. [[CrossRef](#)]
9. Ngao, J.; Cotrufo, M.F. Carbon isotope discrimination during litter decomposition can be explained by selective use of substrate with differing $\delta^{13}\text{C}$. *Biogeosciences* **2011**, *8*, 5–82.
10. Xu, S.; Liu, Y.; Cui, Y.; Pei, Z. Litter decomposition in a subtropical plantation in Qianyanzhou China. *J. For. Res.* **2011**, *16*, 8–15. [[CrossRef](#)]
11. Gautam, M.K.; Lee, K.S.; Song, B.Y.; Lee, D.; Bong, Y.S. Early-stage changes in natural ^{13}C and ^{15}N abundance and nutrient dynamics during different litter decomposition. *J. Plant Res.* **2016**, *129*, 463–476. [[CrossRef](#)]
12. Hobbie, E.A.; Grandy, A.S.; Harmon, M.E. Isotopic and compositional evidence for carbon and nitrogen dynamics during wood decomposition by saprotrophic fungi. *Fungal Ecol.* **2020**, *45*, 100915. [[CrossRef](#)]
13. Hobbie, E.A.; Högberg, P. Nitrogen isotopes link mycorrhizal fungi and plants to nitrogen dynamics. *New Phytol.* **2012**, *196*, 36–382. [[CrossRef](#)] [[PubMed](#)]
14. Kammer, A.; Hagedorn, F. Mineralisation leaching and stabilisation of ^{13}C labelled leaf and twig litter in a beech forest soil. *Biogeosciences* **2011**, *8*, 2195–2208. [[CrossRef](#)]
15. Li, S.G.; Tsujimura, M.; Sugimoto, A.; Davaa, G.; Oyunbaatar, D.; Sugita, M. Temporal variation of $\delta^{13}\text{C}$ of larch leaves from a montane boreal forest in Mongolia. *Trees* **2007**, *1*, 479–490. [[CrossRef](#)]
16. Perakis, S.S.; Sinkhorn, E.R.; Compton, J.E. $\delta^{15}\text{N}$ constraints on long-term nitrogen balances in temperate forests. *Oecologia* **2011**, *167*, 793–807. [[CrossRef](#)] [[PubMed](#)]
17. Preston, C.; Nault, J.; Trofymow, J. Chemical changes during 6 years of decomposition of 11 litters in some Canadian forest sites Part 2 ^{13}C abundance solid-state ^{13}C NMR spectroscopy and the meaning of lignin. *Ecosystems* **2009**, *12*, 1078–1102. [[CrossRef](#)]
18. Du, N.; Zheng, K.; Zhang, J.; Qiu, L.; Zhang, Y.; Wei, X.; Zhang, X. Dual isotopes tracing carbon and nitrogen dynamics during leguminous and non-leguminous litter decomposition under controlled precipitation. *Agronomy* **2023**, *13*, 1205. [[CrossRef](#)]
19. Berg, B.; McLaugherty, C. *Plant Litter: Decomposition, Humus Formation, Carbon Sequestration*, 4th ed.; Springer: New York, NY, USA, 2020.
20. Dijkstra, P.; LaViolette, C.M.; Coyle, J.S.; Doucett, R.R.; Schwartz, E.; Hart, S.C.; Hungate, B.A. ^{15}N enrichment as an integrator of the effects of C and N on microbial metabolism and ecosystem function. *Ecol. Lett.* **2008**, *11*, 389–397. [[CrossRef](#)]
21. Asada, T.; Warner, B.; Aravena, R. Effects of the early stage of decomposition on change in carbon and nitrogen isotopes in Sphagnum litter. *J. Plant Interact.* **2005**, *1*, 229–237. [[CrossRef](#)]
22. Nadelhoffer, K.J.; Fry, B. Nitrogen isotope studies in forest ecosystems. In *Stable Isotopes in Ecology*; Lajtha, K., Michener, R., Eds.; Blackwell Scientific Publications: Oxford, UK, 1994; pp. 22–44.
23. Högberg, P. ^{15}N natural abundance in soil–plant systems. *New Phytol.* **1997**, *137*, 179–203. [[CrossRef](#)]
24. Templer, P.H.; Arthur, M.A.; Lovett, G.M.; Weathers, K.C. Plant and soil natural abundance $\delta^{15}\text{N}$: Indicators of relative rates of nitrogen cycling in temperate forest ecosystems. *Oecologia* **2007**, *153*, 399–406. [[CrossRef](#)] [[PubMed](#)]
25. Melillo, J.M.; Aber, J.D.; Linkins, A.E.; Ricca, A.; Fry, B.; Nadelhoffer, K.J. Carbon and nitrogen dynamics along the decay continuum: Plant litter to soil organic matter. *Plant Soil* **1989**, *115*, 189–198. [[CrossRef](#)]
26. Bragazza, L.; Iacumin, P.; Siffi, C.; Gerdol, R. Seasonal variation in nitrogen isotopic composition of bog plant litter during 3 years of field decomposition. *Biol. Fertil. Soils* **2010**, *46*, 877–881. [[CrossRef](#)]
27. Hobbie, E.A.; Hobbie, J.E. Natural abundance of ^{15}N in nitrogen-limited forests and tundra can estimate nitrogen cycling through mycorrhizal fungi, a review. *Ecosystems* **2008**, *11*, 815–830. [[CrossRef](#)]
28. Osono, T.; Hobara, S.; Koba, K.; Kameda, K.; Takeda, H. Immobilization of avian excreta-derived nutrients and reduced lignin decomposition in needle and twig litter in a temperate coniferous forest. *Soil Biol. Biochem.* **2006**, *38*, 517–525. [[CrossRef](#)]
29. Wedin, D.A.; Tieszen, L.L.; Dewey, B.; Pastor, J. Carbon isotope dynamics during grass decomposition and soil organic matter formation. *Ecology* **1995**, *76*, 1383–1392. [[CrossRef](#)]
30. Benner, R.; Fogel, M.L.; Sprague, E.K. Diagenesis of belowground biomass of *Spartina alterniflora* in salt-marsh sediments. *Limnol. Oceanogr.* **1991**, *36*, 1358–1374. [[CrossRef](#)]
31. Preston, C.M.; Trofymow, J.A.; Flanagan, L.B. Decomposition, $\delta^{13}\text{C}$, and the “lignin paradox”. *Can. J. Soil Sci.* **2006**, *86*, 235–245. [[CrossRef](#)]
32. Fernandez, I.; Mahieu, N.; Cadisch, G. Carbon isotopic fractionation during decomposition of plants materials of different quality. *Glob. Biogeochem. Cycles* **2003**, *17*, 1075. [[CrossRef](#)]
33. Schweizer, M.; Fear, J.; Cadisch, G. Isotopic $\delta^{13}\text{C}$ Fractionation during plant residue decomposition and its implications for soil organic matter studies. *Rapid Commun. Mass Spectrom.* **1999**, *13*, 1284–1290. [[CrossRef](#)]
34. Berg, B.; Booltink, H.G.W.; Breymeyer, A.; Ewertsson, A.; Gallardo, A.; Holm, B.; Johansson, M.-B.; Koivuvoja, S.; Meentemeyer, V.; Nyman, P.; et al. *Data on Needle Litter Decomposition and Soil Climate as Well as Site Characteristics for Some Coniferous Forest Sites*, 2nd ed.; Section 1. Data on site characteristics. Report No 41; Department of Ecology and Environmental Research, Swedish University of Agricultural Sciences: Uppsala, Sweden, 1991.

35. Berg, B.; McClaugherty, C.; Johansson, M.B. *Chemical Changes in Decomposing Plant Litter Can Be Systemized with Respect to the Litter's Initial Chemical Composition*; Reports from the departments in Forest Ecology and Forest Soils; Report 74; Swedish University of Agricultural Sciences: Uppsala, Sweden, 1997.
36. Berg, B.; Berg, M.P.; Bottner, P.; Box, E.; Breymeyer, A.; Calvo de Anta, R.; Couteaux, M.; Gallardo, A.; Escudero, A.; Kratz, W.; et al. Litter mass loss rates in pine forests of Europe and eastern United States: Some relationships with climate and litter quality. *Biogeochemistry* **1993**, *20*, 127–159. [[CrossRef](#)]
37. Jones, J.B., Jr.; Wolf, B.; Mills, H.A. *Plant Analysis Handbook. A Practical Sampling, Preparation, Analysis, and Interpretation Guide*; Micro-Macro Publishing, Inc.: Athens, GA, USA, 1991.
38. Kalra, Y. (Ed.) *Handbook of Reference Methods for Plant Analysis*; CRC Press: Boca Raton, FL, USA, 1997.
39. Campbell, C.R.; Plank, C.O. Preparation of plant tissue for laboratory analysis. In *Handbook of Reference Methods for Plant Analysis*; Kalra, Y., Ed.; CRC Press: Boca Raton, FL, USA, 1998; pp. 37–49.
40. Berg, B.; Booltink, H.G.W.; Breymeyer, A.; Ewertsson, A.; Gallardo, A.; Holm, B.; Johansson, M.-B.; Koivuova, S.; Meentemeyer, V.; Nyman, P.; et al. *Data on Needle Litter Decomposition and Soil Climate as Well as Site Characteristics for Some Coniferous Forest Sites*, 2nd ed.; Section 2. Data on needle litter decomposition. Report No 42. REP 43; Department of Ecology and Environmental Research, Swedish University of Agricultural Sciences: Uppsala, Sweden, 1991.
41. Olson, J.S. Energy storage and the balance of producers and decomposers in ecological systems. *Ecology* **1963**, *44*, 322–331. [[CrossRef](#)]
42. Wieder, R.K.; Lang, G.E. A critique of the analytical methods used in examining decomposition data obtained from litter bags. *Ecology* **1982**, *63*, 1636–1642. [[CrossRef](#)]
43. Berg, B.; Ekbohm, G. Littermass-loss rates and decomposition patterns in some needle and leaf litter types. Long-term decomposition in a Scots pine forest. VII. *Can. J. Bot.* **1991**, *69*, 1449–1456. [[CrossRef](#)]
44. Fry, B. *Stable Isotope Ecology*; Springer: New York, NY, USA, 2006.
45. Fernandez, I.; Cadisch, G. Discrimination against ^{13}C during degradation of simple and complex substrates by two white rot fungi. *Rapid Commun. Mass. Spectrom.* **2003**, *17*, 2614–2620. [[CrossRef](#)] [[PubMed](#)]
46. Hobbie, E.A.; Macko, S.A.; Shugart, H.H. Insights into nitrogen and carbon dynamics of ectomycorrhizal and saprotrophic fungi from isotopic evidence. *Oecologia* **1999**, *118*, 353–360. [[CrossRef](#)] [[PubMed](#)]
47. Boström, B.; Comstedt, D.; Ekblad, A. Isotope fractionation and ^{13}C enrichment in soil profiles during the decomposition of soil organic matter. *Oecologia* **2007**, *153*, 89–98. [[CrossRef](#)] [[PubMed](#)]
48. Blair, N.E.A.L.; Leu, A.; Olsen, J.; Kwong, E.; Des Marais, D. Carbon isotopic fractionation in heterotrophic microbial metabolism. *App. Env. Microbiol.* **1985**, *50*, 996–1001. [[CrossRef](#)]
49. Werth, M.; Kuzyakov, Y. ^{13}C fractionation at the root–microorganisms–soil interface: A review and outlook for partitioning studies. *Soil Biol. Biochem.* **2010**, *42*, 1372–1384. [[CrossRef](#)]
50. Mary, B.; Mariotti, A.; Morel, J.L. Use of ^{13}C variations at natural abundance for studying the biodegradation of root mucilage, roots and glucose in soil. *Soil Biol. Biochem* **1992**, *24*, 1065–1072. [[CrossRef](#)]
51. Wu, J.; Zhang, Q.; Yang, F.; Zhang, Q.; Cheng, X. Does short-term litter input manipulation affect soil respiration and its carbon-isotopic signature in a coniferous forest ecosystem of central China? *Appl. Soil Ecol.* **2017**, *113*, 45–53. [[CrossRef](#)]
52. Šantrůčková, H.; Bird, M.I.; Lloyd, J. Microbial processes and carbon-isotope fractionation in tropical and temperate grassland soils. *Funct. Ecol* **2000**, *14*, 108–114. [[CrossRef](#)]
53. Bragazza, L.; Iacumin, P. Seasonal variation in carbon isotopic composition of bog plant litter during 3 years of field decomposition. *Biol. Fertil. Soils* **2009**, *46*, 73–77. [[CrossRef](#)]
54. Benner, R.; Fogel, M.L.; Sprague, E.K.; Hodson, R.E. Depletion of ^{13}C in lignin and its implications for stable carbon isotope studies. *Nature* **1987**, *329*, 708–710. [[CrossRef](#)]
55. Hall, S.J.; Huang, W.; Timokhin, V.I.; Hammel, K.E. Lignin lags, leads, or limits the decomposition of litter and soil organic carbon. *Ecology* **2020**, *101*, e3113. [[CrossRef](#)] [[PubMed](#)]
56. Berg, B.; Staaf, H. Decomposition rate and chemical changes of Scots pine needle litter. II. Influence of chemical composition. *Ecol. Bullet.* **1980**, *32*, 373–390.
57. Hobbie, E.A.; Macko, S.A.; Williams, M. Correlations between foliar $\delta^{15}\text{N}$ and nitrogen concentrations may indicate plantmycorrhizal interactions. *Oecologia* **2000**, *122*, 273–283. [[CrossRef](#)]
58. Knorr, M.; Frey, S.D.; Curtis, P.S. Nitrogen additions and litter decomposition: A meta-analysis. *Ecology* **2005**, *86*, 3252–3257. [[CrossRef](#)]
59. Talbot, J.M.; Treseder, K.K. Interactions among lignin, cellulose, and nitrogen drive litter chemistry–decay relationships. *Ecology* **2012**, *93*, 345–354. [[CrossRef](#)]
60. Chen, J.; Luo, Y.; van Groenigen, K.J.; Hungate, B.A.; Cao, J.; Zhou, X.; Wang, R. A keystone microbial enzyme for nitrogen control of soil carbon storage. *Sci. Adv.* **2018**, *4*, eaaq1689. [[CrossRef](#)]
61. Berg, B.; Söderström, B. Fungal biomass and nitrogen in decomposing Scots pine needle litter. *Soil Biol. Biochem.* **1979**, *11*, 339–341. [[CrossRef](#)]
62. Myers, R.J.K.; Palm, C.A.; Cuevas, E.; Gunatilleke, I.U.N.; Brossard, M. The synchronization of nutrient mineralization and plant nutrient demand. In *The Biological Management of Tropical Soil Fertility*; Woomer, P.L., Swift, M.J., Eds.; John Wiley and Sons: Chichester, UK, 1994; pp. 81–116.

-
63. Kramer, M.G.; Sollins, P.; Sletten, R.S.; Swart, P.K. N isotope fractionation and measures of organic matter alteration during decomposition. *Ecology* **2003**, *84*, 2021–2025. [[CrossRef](#)]
 64. Hogberg, M.N.; Hogberg, P.; Myrold, D.D. Is microbial community composition in boreal forest soils determined by pH, C-to-N ratio, the trees, or all three? *Oecologia* **2007**, *150*, 590–601. [[CrossRef](#)] [[PubMed](#)]

Disclaimer/Publisher’s Note: The statements, opinions and data contained in all publications are solely those of the individual author(s) and contributor(s) and not of MDPI and/or the editor(s). MDPI and/or the editor(s) disclaim responsibility for any injury to people or property resulting from any ideas, methods, instructions or products referred to in the content.